Scattering From a Partially Coated Shell Immersed in Water Using a Subtractive Modelling Technique

F. Dumortier, V. Meyer, Laurent Maxit

Journal of Theoretical and Computational Acoustics

Scattering from a partially coated shell immersed in water using a subtractive modelling technique

F. Dumortier
Univ Lyon, INSA Lyon, LVA, EA677,
25 bis av. Jean Capelle, 69621 Villeurbanne Cedex, France
florent.dumortier@insa-lyon.fr

V. Meyer
Naval Group,
199 av. Pierre-Gilles de Gennes, 83190 Ollioules, France
valentin.meyer@naval-group.com

L. Maxit
Univ Lyon, INSA Lyon, LVA, EA677,
25 bis av. Jean Capelle, 69621 Villeurbanne Cedex, France
laurent.maxit@insa-lyon.fr

In this study, we focus on the prediction of the pressure field scattered from an immersed cylindrical shell partially coated by a soft rubber, impacted by an acoustic plane wave. As the coating covers only a partial portion along the circumference of the shell, the considered system is not axisymmetric. As a result, a spectral (Fourier) resolution of the mathematical problem would induce the coupling of the different circumferential orders, which can lead to prohibitive computing times. To circumvent this issue, the reverse Condensed Transfer Function (rCTF) method has recently been developed to decouple vibroacoustic subsystems initially coupled along lines or surfaces. From an analytical model of the fully coated shell impacted by the acoustic plane wave and a finite element (FE) model of the missing coating material, the rCTF approach predicts the vibroacoustic behavior of the coated shell with a voided section instead of the removed part. This voided section can then be filled by a FE model of the water domain replacing the removed coating material, using the direct CTF approach. The principle of the rCTF approach, some numerical validations, and results for the scattering from the partially coated shell are presented in this paper.

Keywords: Vibroacoustic; Subtractive modelling; Acoustic scattering ; Numerical methods; Cylindrical shells.

1. Introduction

Studying the vibroacoustic performances of cylindrical shells finds great interest for industrial applications. They are particularly used in the naval context, in order to model hulls of underwater vehicles. Indeed, acoustic performances of underwater vehicles must be predicted in a large frequency range following the increasing capabilities of Sonar antennas. In order to enhance the vibroacoustic performances of underwater vehicles, acoustic coatings can be applied at the surface of the hull. Those coatings are generally made of soft material and can mainly be divided into two categories. Decoupling coatings are used to reduce the

radiation by decoupling the hull from the external fluid medium. On the other hand, anechoic coatings are used to limit the scattering from the hull by absorbing incoming waves thanks to their impedance match with water.[1]

Over the past decades, a substantive amount of work has been produced to study such technologies and how well they contribute to the mitigation of the noise produced by the structure they are mounted on. Several approaches to model the coating have been investigated, among which we can cite the locally reacting material approach convenient for the simpleness of its implementation. Locally reacting materials have been used to study radiation[2] and scattering[3] from cylindrical shells, but it was observed that this theory is limited in a physical point of view, mainly because it is unable to describe the behavior of the coating in its thickness. A second, more robust, theory is to model the coating using the three-dimensional theory of elasticity.[4,5] This approach gives better results as it accounts for both longitudinal and shear waves travelling in the material, with the main drawback of being much more time consuming. A third approach consists in modelling the coating as an equivalent fluid, meaning that only the longitudinal waves are accounted for in the coating.[6] This approach, particularly indicated when the coating is made of soft material, is a good compromise between the two aforementioned approaches, as it has proven to better capture the physical phenomena in the coating than the locally reacting approach, while being less computationally intensive than the three-dimensional theory of elasticity.

While only the case of homogeneous media has been discussed here, heterogeneous coatings also have been studied in literature. In particular, cylindrically layered media can show great interest as they could allow for example overlaying anechoic and decoupling coatings. A mathematical framework to study cylindrically layered media infinite along the axial direction has been presented by Skelton and James.[1] It is based on a spectral approach where the equations of motion of the shell are solved in the wavenumber domain, by the means of a Fourier transform along the length of the shell and a Fourier series decomposition along its circumference. A global matrix assembly procedure is then used to account for several kinds of layers, which can either be solid or fluid,[7] allowing extending the classical Transfer Matrix Method for so-called *large fd* problems (i.e. at high wavenumber-thickness product) where high numerical instabilities occur. Heterogeneous coatings formed with resonant inclusions have also been studied as way to improve the sound absorption by the coating, either in terms of performances or frequency range. In particular, coatings constituted by a matrix of soft rubber with void inclusions,[6] hard inclusions[8] or both void and hard inclusions[9] have been investigated using analytical homogenisation theories. The previously cited studies were focused on the material technology in itself, but its influence when mounted on a cylindrical shell has also been studied.[10] Other theories can be used such as the layer-multiple-scattering method, which allows to consider the double-periodic problem of anechoic coatings with periodic cavities as a 2-D case because of the invariance in axial direction.[11–13]

If those studies focus on fully coated cylindrical shells, less attention has been paid to the study of partially coated cylindrical shells. Studying such coating configurations can find physical or practical interests, for example to study the impact of a missing coating tile on

the vibroacoustic behavior of the system, or to account for areas where the shell is covered with anechoic coating, and other areas where the shell is covered with decoupling coating. However, a difficulty arises from the loss of axisymmetry induced by the partial coating. Indeed, the spectral procedure described in[1] is based on the assumption of axisymmetry of the system. Hence, the only studies focused on partial coating are restricted to the locally reacting material approach to describe the coating.[3,14,15]

On the other hand, from a numerical point of view, substructuring methods have emerged during the past decades to overcome the frequency limitations of element-based methods such as the Finite Element Method (FEM). They allow studying rather complex systems by separating them into simpler subsystems which can be studied separately, before coupling the subsystems by the means of frequency transfer functions. In particular, substructuring methods based on admittance and impedance concepts will be of interest here. In the Patch Transfer Function (PTF) method,[16] the interface between the subsystem is separated into a number of elementary surfaces called patches, and computing the transfer functions between the patches for each subsystem allows coupling them together. This approach has proved to be popular in the automotive industry,[16–18] but has found applications in other kind of industries, such as the naval industry[19,20] to study the transmission of sound through the ballasts of a submarine vessel. Still initially focused for naval applications, the Circumferential Admittance Approach (CAA)[21] has been developed to couple a model of a cylindrical shell immersed in water to axisymetric internal structures such as stiffeners or bulkheads. In this method, the fluid-loaded cylindrical shell is studied using the spectral procedure described in.[1] This method has then been applied to study the scattering from a stiffened cylindrical shell.[22] Later on, the principle of the method was extended to non-axisymetric internal frames such as floors or engine foundations by the way of the Condensed Transfer Function (CTF) method, to investigate their contribution on radiation and scattering from the shell.[23–25] As such, the CTF method can be seen as a generalisation of both the PTF and CAA methods.

Following these recent advances, the reverse Condensed Transfer Function (rCTF) has been developed as a reverse formulation of the CTF method to decouple subsystems initially coupled along lines or surfaces. One of the main advantages of these methods is that it allows to study non-axisymetric systems, proving an interesting potential to address the issue of the partially coated cylindrical shell. The mathematical framework of the method was proposed in,[26] while the procedure to compute the so-called Condensed Transfer Functions (necessary to apply the method) from numerical models has been described in.[27] A global approach of subtractive modelling was then proposed to improve the convergence of the method by extending the definition of the decoupling interface to interior boundaries of the initial system.[28] This paper is focused on addressing the problem of the scattering of an incident plane wave by a partially coated cylindrical shell, by using a coupled CTF-rCTF approach. Hence, the rCTF formulation is extended to predict the pressure field scattered by a partially coated cylindrical shell. The theoretical framework is presented in Section 2, whereas the numerical processes used to evaluate the condensed transfer functions are addressed in Section 3. The numerical results of the proposed approach concerning the

scattering from the partially coated shell immersed in water are then discussed in Section 4, before concluding this paper.

2. Principle of the coupled CTF-rCTF method

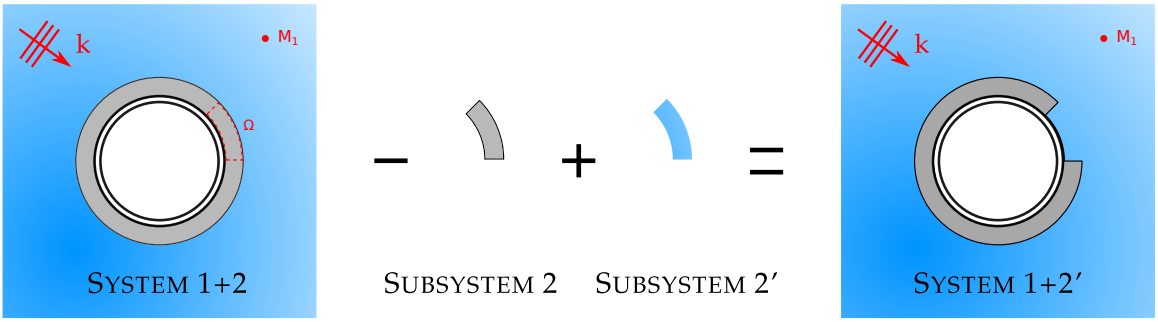

Figure 1. Studying a partially coated cylindrical shell. The '-' sign illustrates the rCTF method; the '+' sign illustrates the CTF method.

In order to study the scattering from a partially coated cylindrical shell, the coupled CTF-rCTF method, illustrated in Figure 1, is applied. It consists in considering initially a model of the fully coated cylindrical shell impinged by a harmonic acoustic plane wave (system 1+2 in Figure 1). From this system, a model of the missing part of the coating (subsystem 2 in Figure 1) is removed. This first operation, called the decoupling procedure, is performed using the rCTF method and is illustrated in Figure 2. This results in an intermediary subsystem: the partially coated cylindrical shell, for which the missing part of the coated has been replaced by a rigid void (subsystem 1 in Figure 2, where the white area correponds to the void). Then the obtained subsystem is coupled to a model of the water domain replacing the removed coating material (subsystem 2' in Figure 1). This second operation is called the recoupling procedure, is performed using the CTF method and is illustrated in Figure 3. The obtained system is finally the partially coated cylindrical shell immersed in water (system 1+2' in Figure 1) impacted by the harmonic acoustic plane wave. In the following sections, the mathematical frameworks for the decoupling and recoupling procedures will be recalled.

2.1. *Decoupling procedure using the rCTF method*

In order to consider the decoupling problem (Figure 2), the rCTF method is used. The theoretical fundamentals of this procedure have been explained in details in reference,[26] but the main steps will be recalled here.

For the sake of conciseness, a 2D model of our system is considered. Let us consider two systems initially coupled along a line Ω. The system 1+2, corresponding to the fully coated cylindrical shell, is excited by an external acoustic plane wave, and the responses are

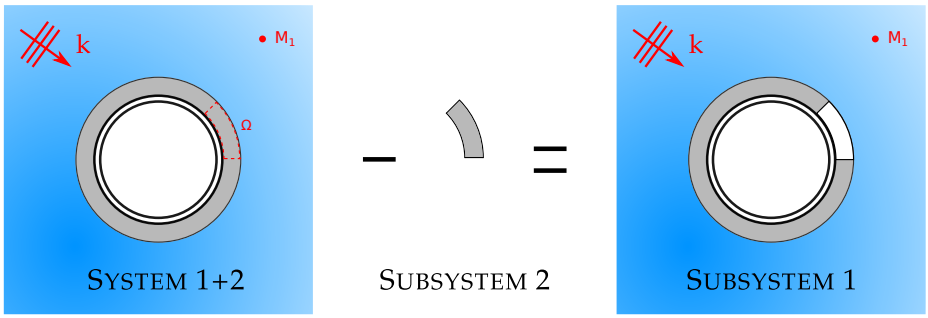

Figure 2. Decoupling procedure using the rCTF method.

calculated in harmonic regime. The objective of this decoupling procedure is to obtain the response at any point M_1 of subsystem 1. To this end, a set of N orthonormal functions, called condensation functions, is defined on Ω: $\{\varphi^i\}_{1\leqslant i\leqslant N}$. Then, the pressures p_α and normal velocities u_α on Ω can be approximated, for each (sub)system α, as a linear combination of the condensation functions

$$p_\alpha(x) \simeq \sum_{i=1}^{N} P_\alpha^i \varphi^i(x) \quad \text{and} \quad u_\alpha(x) \simeq \sum_{i=1}^{N} U_\alpha^i \varphi^i(x), \quad x \in \Omega \tag{1}$$

where P_α^i and U_α^i are the unknowns. They can be estimated by defining, for each uncoupled subsystem (i.e. subsystems 1 and 2), condensed transfer functions (CTFs) between φ^i and φ^j. These CTFs are defined by applying a prescribed velocity $u_\alpha = \varphi^j$ on Ω, meaning that the CTFs will result in condensed impedances

$$Z_\alpha^{ij} = \frac{\langle \bar{p}_\alpha, \varphi^i \rangle}{\langle u_\alpha, \varphi^j \rangle} = \langle \bar{p}_\alpha, \varphi^i \rangle \tag{2}$$

where $\langle f, g \rangle = \int f(x) g^*(x)\, \mathrm{d}x$ (with * denoting the complex conjugate), and $\bar{p}_\alpha$ corresponds to the resulting pressure on Ω when the subsystem is excited by $u_\alpha = \varphi^j$. Concerning system 1+2, as the decoupling boundary Ω is a fictitious one, a prescribed velocity jump corresponding to φ^j must be considered to define its condensed impedances

$$Z_{1+2}^{ij} = \frac{P_{1+2}^i}{\delta U_{1+2}^j} = \frac{\langle \bar{p}_{1+2}, \varphi^i \rangle}{\langle \varphi^j, \varphi^j \rangle} = \langle \bar{p}_{1+2}, \varphi^i \rangle \tag{3}$$

The condensed impedances are calculated for each couple of condensation functions for each system/subsystem. The condensed impedance matrix for system/subsystem α can subsenquently be defined as $\boldsymbol{Z_\alpha} = \left[Z_\alpha^{ij} \right]_{N \times N}$. Then, following some developments of the rCTF approach described in reference,[26] the condensed impedance matrix of subsystem 1 can be obtained from the condensed impedance matrices of system 1+2 and subsystem 2:

$$\boldsymbol{Z_1} = \boldsymbol{Z_2}\left(\boldsymbol{Z_2} - \boldsymbol{Z_{1+2}}\right)^{-1}\boldsymbol{Z_{1+2}} \tag{4}$$

The contribution from the plane wave excitation must be introduced through the definition of the free condensed pressures of the system 1+2

$$P^i_{1+2} = \langle p_{1+2}, \varphi^i \rangle \tag{5}$$

where p_{1+2} is the pressure induced by the acoustic plane wave on the the decoupling boundary Ω. Then, to estimate the response at any point M_1 of the uncoupled subsystem 1, the quantity $Z^i_{1+2}(M_1)$, corresponding to the response at point M_1 in the system 1+2 when Ω is excited by a velocity jump φ^i, must be introduced. This quantity can be inferred from the free condensed pressures induced by a monopole of unit volume velocity located at point M_1, using a reciprocity principle[29,30]

$$Z^i_{1+2}(M_1) = P^{M_1 i\,*}_{1+2} = \langle p^{M_1 *}_{1+2}, \varphi^i \rangle^* \tag{6}$$

where $p^{M_1 *}_{1+2}$ is the complex conjugate of the pressure induced on the decoupling boundary Ω by a monopole of unit volume velocity located at point M_1. It must be underlined that the introduction of the complex conjugates in Eq. 6 comes from the use of the reciprocity principle. Indeed, the complex conjugate of the condensation function must appear in the definition of a condensed quantity, which is not the case when using the reciprocity principle, leading to the necessity of adding the complex conjugates to have a correct correlation between the different quantities. The condensed pressure vectors of system 1+2 can subsequently be defined as $\boldsymbol{P_{1+2}} = \left[P^i_{1+2}\right]_{N\times 1}$ and $\boldsymbol{P^{M_1 *}_{1+2}} = \left[P^{M_1 i\,*}_{1+2}\right]_{N\times 1}$. Finally, the pressure at any point M_1 of the uncoupled subsystem 1 can be written as

$$p_1(M_1) = p_{1+2}(M_1) + \left(\left(\boldsymbol{I} + \boldsymbol{Z_1}\boldsymbol{Z_2}^{-1}\right)\boldsymbol{P^{M_1 *}_{1+2}}\right)^T \boldsymbol{Z_2}^{-1}\boldsymbol{P_{1+2}} \tag{7}$$

where $p_{1+2}(M_1)$ is the pressure induced by the acoustic plane wave at point M_1 of system 1+2.

2.2. *Recoupling procedure using the CTF method*

Once the pressure has been obtained in the decoupled subsystem 1, we are interested in recoupling this subsystem to a water tile occupying the missing part of the coating material, to obtain the partially coated cylindrical shell (Figure 3). The recoupling procedure is performed using the CTF method, for which the theoretical fundamentals have been developed in[26] for acoustical systems and in[24] for mechanical systems.

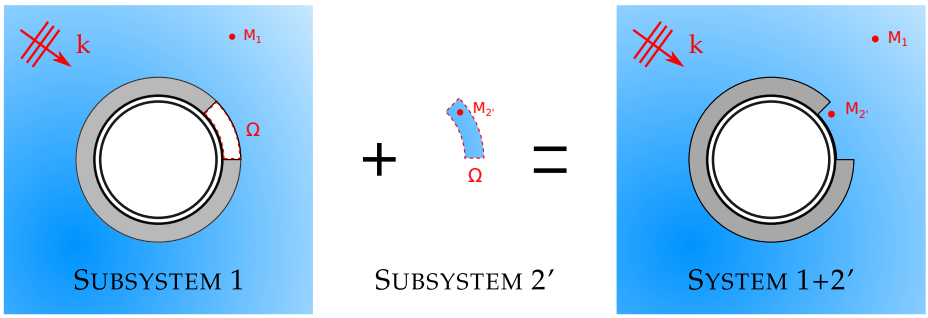

Figure 3. Recoupling procedure using the CTF method.

We can find the pressure at any point of the coupled system 1+2', for which the expression depends if the considered point initially belonged to subsystem 1 or subsystem 2'

$$\begin{cases} p_{1+2'}(M_1) = \tilde{p}_1(M_1) + \mathbf{Z_1}^T(M_1)\mathbf{U_{1+2'}} & \text{(8a)} \\ p_{1+2'}(M_{2'}) = -\mathbf{Z_{2'}}^T(M_{2'})\mathbf{U_{1+2'}} & \text{(8b)} \end{cases}$$

where the point M_1 initially belongs to subsystem 1, while the point $M_{2'}$ initially belongs to subsystem 2'. $\mathbf{Z_1}(M_1)$ is the vector of the point condensed impedances of subsystem 1, and its components are defined similarly as $Z^i_{1+2}(M_1)$, using a reciprocity principle.[29,30] The vector can then be expressed as[26]

$$\mathbf{Z_1}(M_1) = \mathbf{P_1^{M_1}}^* = \left(\mathbf{I} + \mathbf{Z_1}\mathbf{Z_2}^{-1}\right)\mathbf{P_{1+2}^{M_1}}^* \tag{9}$$

Concerning $\mathbf{U_{1+2'}}$, it reads

$$\mathbf{U_{1+2'}} = -\left(\mathbf{Z_1} + \mathbf{Z_{2'}}\right)^{-1}\tilde{\mathbf{P}}_\mathbf{1} \tag{10}$$

As $\mathbf{Z_1}$ has already been computed, the necessary quantities here are $\mathbf{Z_{2'}}$ (which is assumed to be known), and $\tilde{\mathbf{P}}_\mathbf{1}$. The latter corresponds to the condensed pressure at the surface Ω of the uncoupled subsystem 1 when the excitation is the acoustic plane wave and can then be noted $\tilde{\mathbf{P}}_\mathbf{1}$. It is calculated in a similar way as $\tilde{\mathbf{P}}_\mathbf{1}^{\mathbf{M_1}}$ in Equation 9

$$\tilde{\mathbf{P}}_\mathbf{1} = \left(\mathbf{I} + \mathbf{Z_1}\mathbf{Z_2}^{-1}\right)\mathbf{P_{1+2}} \tag{11}$$

From these information, Eq. 8a can be rewritten

$$p_{1+2'}(M_1) = p_{1+2}(M_1) + \left(\left(\mathbf{I} + \mathbf{Z_1}\mathbf{Z_2}^{-1}\right)\mathbf{P_{1+2}^{M_1}}^*\right)^T\left(\mathbf{Z_2}^{-1}\mathbf{P_{1+2}} - \left(\mathbf{Z_1} + \mathbf{Z_{2'}}\right)^{-1}\tilde{\mathbf{P}}_\mathbf{1}\right) \tag{12}$$

where $\mathbf{Z_1}$ and $\tilde{\mathbf{P}}_\mathbf{1}$ are expressed from Eqs. 4 and 11, respectively. On the other hand, Eq. 8b gives

$$p_{1+2'}(M_{2'}) = \mathbf{Z_{2'}}^T(M_{2'})\left(\mathbf{Z_1} + \mathbf{Z_{2'}}\right)^{-1}\tilde{\mathbf{P}}_\mathbf{1} \tag{13}$$

where $\mathbf{Z_{2'}}(M_{2'})$ can be computed by evalutating the pressure at point $M_{2'}$ of subsystem 2' when the excitation is a condensation function.

From Eqs. 12 and 13, the pressure scattered by the partially coated cylindrical shell can be estimated at any point in the fluid domain, from the condensed impedances of the fully coated shell (i.e. system 1+2), of the removed coating patch (i.e. subsystem 2) and of the added water domain (i.e. subsystem 2'). In the next section, we are going to focus on the numerical computation of these condensed impedances ($\mathbf{Z_{1+2}}$, $\mathbf{Z_2}$ and $\mathbf{Z'_2}$).

3. Numerical calculation of the condensed impedances

In order to apply the process proposed in Section 2, the condensed impedance matrices $\mathbf{Z_{1+2}}$, $\mathbf{Z_2}$ and $\mathbf{Z'_2}$ must be computed. After a preliminary introduction of the considered system and of the condensed transfer functions in subsection 3.1, the procedure to evaluate numerically the condensed impedances will be developed in subsections 3.2 and 3.3 for the system 1+2 and subsystems 2 and 2', respectively.

3.1. *Description of the system and of the condensation functions*

In the following, we consider a cylindrical shell of radius R, thickness h, Young's modulus E_s, density ρ_s and Poisson's ratio ν_s. It is excited by a harmonic acoustic plane wave of oblique incidence θ^i compared to the vertical direction (see Figure 4a). The behavior of the shell are described using Flügge equations for thin shells.[31]

The coating is an anechoic coating of thickness h_p and density ρ_p, and will be modelled as an equivalent fluid, meaning that the transverse waves travelling in the coating are not taken into account. The celerity of longitudinal waves in the coating is noted c_p, while its damping loss factor is η_p. The acoustic properties of the coating correspond to the ones used for the BeTSSi II (Benchmarking of Target Strength Simulations) international workshop.[32] The coated shell is surrounded by a fluid medium of density ρ_f and speed of sound c_f, and a damping loss factor η_f is introduced to avoid numerical instabilities.[26] Both fluid domains are modelled using the Helmholtz equation, and the Sommerfeld radiation condition is verified at infinity

$$\begin{cases} \Delta p(r,\theta,x) + k_f^2 p(r,\theta,x) = 0 \\ \lim\limits_{r\to\infty} r\left(\mathrm{j}k_f p + \frac{\partial p}{\partial r}\right) = 0 \end{cases} \tag{14}$$

where k_f is the acoustic wavenumber.

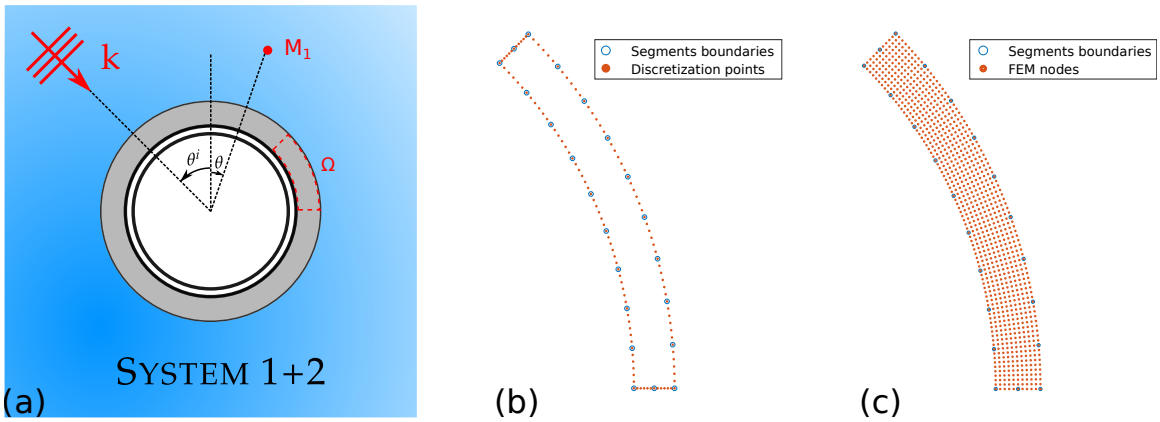

Figure 4. (a) Fully coated cylindrical shell impacted by an acoustic plane wave. (b) Discretization of the decoupling boundary for the system 1+2. (c) FE model for the subsystem 2.

Besides, the continuity of normal velocities and pressures are considered at the shell-coating and coating-exterior fluid interfaces. The characteristics of the shell, the coating and the surrounding fluid domain are presented in Table 3.1. It must be stressed that, in the following, the computations are carried out using 2D models. This choice was made in order to be able to compare the obtained results to a FEM reference calculation. Therefore, the oblique incidence of the acoustic plane wave in the azimuthal plane was not taken into account.

Table 1. Material and fluids characteristics.

Parameter	Notation	Value	Unit
Shell radius	R	1	m
Shell thickness	h_s	0.01	m
Shell Young's modulus	E_s	210	GPa
Shell Poisson's ratio	ν_s	0.3	-
Shell density	ρ_s	7800	kg.m^{-3}
Shell damping loss factor	μ_s	0.01	-
Coating thickness	h_p	0.1	m
Coating density	ρ_p	1600	kg.m^{-3}
Coating speed of sound	c_p	841.5	m.s^{-1}
Coating loss factor	μ_p	0.236	-
Exterior fluid density	ρ_f	1000	kg.m^{-3}
Exterior fluid speed of sound	c_f	1500	m.s^{-1}
Exterior fluid loss factor	μ_f	0.001	-

In this work, as the decoupling boundary Ω is a 1D one (because we are working with 2D models), the condensation functions are chosen to be gate functions. This means that the decoupling boundary Ω, of length Γ, is divided into N segments. The condensation

functions are then defined depending on their length L_s

$$\varphi^i(s) = \begin{cases} \frac{1}{\sqrt{L_s}} & \text{if} \quad (i-1)L_s \leqslant s < iL_s \\ 0 & \text{elsewhere} \end{cases}, \quad i \in [\![1, N]\!] \quad 0 \leqslant s \leqslant \Gamma \tag{15}$$

The size of the segments follows a wavelength-based criterion, and must be smaller than half the minimal wavelength (between the acoustic wavelength in the surrounding fluid, the acoustic wavelength in the coating and the flexural wavelength of the shell) at the highest considered frequency. In the following, the calculations are carried out between 5 Hz and 1500 Hz. At this frequency, the acoustic wavelength in the coating is the smaller one, and is then the one retained to define the size of the segments. Following this criterion, the decoupling boundary Ω is divided into 22 segments as illustrated in Figure 4b.

3.2. *Condensed impedances of the fully coated cylindrical shell*

According to the definition of the condensed impedances given in Eq. 3, a velocity jump must be applied on the decoupling boundary and the resulting pressure must be calculated. Besides, to correspond to a condensation function, the velocity jumps will be applied successively on each segment of the decoupling boundary according to Eq. 15. To emulate these velocity jumps, an integral formulation derived from the indirect BEM formulation is retained. Following this formulation, the pressure field from a radiating surface can be expressed as

$$p(M) = \int_\Omega \nu(P) G(M,P)\, \mathrm{d}\Omega(P), \quad M \in \Omega, \quad P \in \Omega \tag{16}$$

where $\nu(P)$ is the single layer potential due to a layer of monopole sources and represents a velocity jump at the crossing of Ω. It can be expressed from the velocity jump δU as

$$\nu(P) = \mathrm{j}\omega\rho_f \delta U(P) \tag{17}$$

$G(M,P)$ is the free-field Green function and corresponds to the pressure at point M due to a monopole source located at point P

$$G(M,P) = -\frac{\mathrm{e}^{\mathrm{j}k_f(1-\mathrm{j}\eta_f)|M-P|}}{4\pi|M-P|} \tag{18}$$

with $|M-P|$ being the Euclidian distance between the two points. According to the definition of the single layer potential, the velocity jump can then be emulated by placing on Ω an array of monopole sources, which allows to evaluate numerically the integral in Eq. 16.

In practice, the formulation to obtain the pressure induced at a single point by a monopole excitation must be derived. This calculation is done via a semi-analytical approach in the wavenumber domain as described in,[1] by the means of a Fourier series decomposition

along the circumferential coordinate. It is worth mentioning that, if we were to work with 3D models, a Fourier transform along the axial coordinate would also be performed. Finally, the total pressure at a single point n_i due to a monopole excitation located at point n_j can be retrieved by adding the contribution of all the circumferential orders

$$p_{tot}^{n_i n_j} = \sum_{n=-\infty}^{n=+\infty} \tilde{p}_{tot}^{n_i n_j} \mathrm{e}^{\mathrm{j}n\theta_{n_i}} \tag{19}$$

where $\tilde{p}_{tot}^{n_i n_j}$ is the total spectral pressure obtained using the procedure in.[1] The sum in Eq. 19 is theoretically infinite, but is in practice truncated to a finite value N_{max} derived from the maximal value of the different wavenumbers of the problem,

$$N_{max} = \mathrm{int}\left[\kappa_n R \max(k_f, k_p, k_s)\right] \tag{20}$$

with k_f the acoustical wavenumber in the surrounding fluid medium, k_p the acoustical wavenumber in the anechoic coating, and k_s the flexural wavenumber of the shell. κ_n is a margin coefficient generally fixed to 1.5 for such problems.

The condensed impedance between the incident segment j and the receiving segment i is then obtained by summing the resulting pressures at all the points N_i belonging to the segment i, due to monopole excitations on all the points N_j belonging to the segment j

$$Z_{1+2}^{ij} = \sum_{n_i=1}^{N_i} \sum_{n_j=1}^{N_j} \frac{p_{tot}^{n_i n_j}}{\sqrt{L_j L_i}} \delta\xi_j \delta\xi_i \tag{21}$$

where L_i and L_j are the length of the segments i and j, respectively, and $\delta\xi_i$ and $\delta\xi_j$ correspond to the discretization step in the segments (which depends on the location of the segment on the decoupling boundary).

It must be emphasized that the expression of the pressure in Eq. 12 also relies on the calculation of the condensed pressures $\mathbf{P_{1+2}}$ and $\mathbf{P_{1+2}^{M_1}}$. These condensed pressures are numerically evaluated in a similar way as $\mathbf{Z_{1+2}}$, in the sense that the expressions of the pressure induced by the acoustic plane wave (for $\mathbf{P_{1+2}}$) and by the unit monopole (for $\mathbf{P_{1+2}^{M_1}}$) are projected on the segments using the discretization points. The details of these calculations will not be addressed here, but they can be found in.[33]

3.3. *Condensed impedances of the missing coating material and the water patch*

Concerning the condensed impedances of the missing coating material and of the water patch added to fill up the voided section, they must be computed by applying a prescribed velocity on the decoupling boundary, as defined in Eq. 2. To do so, and given the small size of the subsystem, a Finite Element (FE) formulation was used. An example of the FE

model of the removed patch can be seen in Figure 4c. As we are working here with acoustical systems, the FEM formulation which must be solved yields

$$\left([\mathbf{K}] - \omega^2 [\mathbf{M}] (1 - 2\mathrm{j}\eta)\right) \{\mathbf{P}\} = \{\mathbf{Q}\} \tag{22}$$

where $[\mathbf{K}]$ and $[\mathbf{M}]$ are the acoustic stiffness and mass matrices, respectively, η is the damping loss factor (either in the coating or in the surrounding fluid), $\{\mathbf{P}\}$ is the output pressure vector, and $\{\mathbf{Q}\}$ is the input volume velocity vector.

The procedure to compute the condensed impedances of the subsystems is then similar to the one described in subsection 3.2. The nodes of the FE model are firstly associated to the different segments to which they belong, in order to define the condensation functions. Then, a volume velocity excitation is applied on the nodes belonging to the incident segment j according to the definition of the condensation functions in Eq. 15. Following this, the input volume velocity vector $\{\mathbf{Q^j}\}$ associated to the incident segment j will have N_j non-null components Q_n^j, with N_j being the number of nodes belonging to the segment j

$$Q_n^j = \frac{\delta S_n}{\sqrt{L_j}}, \quad n \in [\![1, N_j]\!] \tag{23}$$

where δS_n is the length around the node n, and L_j the length of the segment j. The resulting pressure vector $\{\mathbf{P^j}\}$ of the FE model is then obtained by inverting directly the dynamic matrix of Eq. 22. This operation is not computationally costly as the system has a low number of degrees of freedom.

$$\{\mathbf{P^j}\} = \left([\mathbf{K}] - \omega^2 [\mathbf{M}] (1 - 2\mathrm{j}\eta)\right)^{-1} \{\mathbf{Q^j}\} \tag{24}$$

Finally, the condensed impedance between the incident segment j and the receiving segment i is obtained by summing the resulting pressure at all the M_i nodes belonging to the receiving segment

$$Z_\alpha^{ij} = \frac{1}{\sqrt{L_i}} \sum_{m=1}^{M_i} P_m^j \delta S_m \tag{25}$$

where P_m^j is the pressure at node m belonging to the segment i when the system is excited on the segment j, δS_m is the length around the node m, L_i is the length of the segment i, and α corresponds either to subsystem 2 or subsystem 2'.

4. Scattering from the partially coated shell immersed in water

In Section 3, the formulations to obtain the necessary quantities have been demonstrated. We can now proceed with the application of the method to predict the scattering from the partially coated cylindrical shell impacted by a plane wave of unit amplitude, for which

the missing coating part spreads from 0 to $\pi/4$ as illustrated in Figure 5. Two loading configurations will be considered. In the first one, the acoustic plane wave will be incident on the uncoated part of the shell, while for the second one, the acoustic plane wave will impinge the other side of the shell.

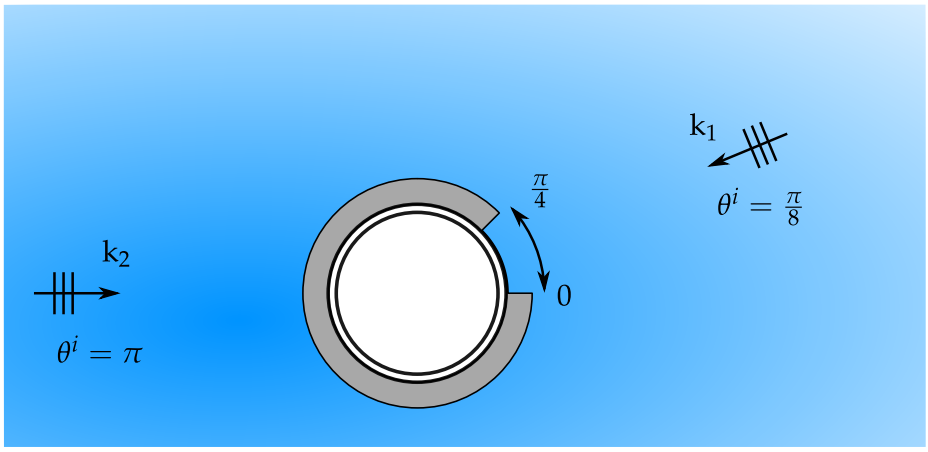

Figure 5. Loading cases and angular spreading of the partial coating.

A first paragraph will be dedicated to address some theoretical aspects of the scattering problem, in order to understand the quantities that will be studied hereafter. Then, we will be interested in investigating the impact of partial coating on the near-field and far-field scattered pressure.

4.1. *Theoretical aspects concerning the scattering problem*

When dealing with the scattering problem, the total pressure in the domain can be decomposed as three different components: the incident pressure p_{inc} corresponding to the pressure induced by the acoustic plane wave, the reflected pressure p_{refl} corresponding to the pressure scattered as though the boundary were hard, and the reradiated pressure p_{rad} stemming from the cylinder motion. Generally, when the scattering problem is considered, the contribution of the elastic part (i.e. the reradiated pressure) is studied separately from the contribution of the rigid part (i.e. the sum of the incident and reflected pressure, also called the blocked pressure). This can be summarized in Eq. 26[1]

$$p = \underbrace{p_{inc} + p_{refl}}_{p_{block}} + p_{rad} \tag{26}$$

In the following, we will be interested into evaluating the reradiated pressure by the cylindrical shell. Indeed, one must keep in mind that the problem investigated here constitutes a first step towards the study of 3D partially coated, stiffened cylindrical shells.

For such studies, we can be interested in the elastic component of the scattered pressure (i.e. p_{rad}) as the spectra of monostatic backscattered pressures show patterns of periodic discontinuities (namely Bragg scattering and scattering from Bloch-Floquet waves) arising from the interaction between the incident wave and the elastic stiffeners.[22,34]

To obtain the pressure reradiated by the partially coated shell, we have seen in Eq. 12 that the first step is to compute the pressure reradiated by the fully coated shell, $p_{1+2}(M_1)$. The procedure to obtain this reradiated pressure is not trivial and will be developed here.

Let us consider the problem presented in Figure 4a. The calculation is performed in two steps. The first one consists in solving the blocked pressure problem, i.e. the response of the system when the shell is considered as rigid. The blocked pressure at the surface of the shell is then used as an excitation term to derive the radial displacement of the shell and ultimately the reradiated pressure. The blocked pressure satisifies the following conditions

- Helmholtz equation with a source term in the exterior fluid domain,
- homogeneous Helmholtz equation in the coating,
- Sommerfeld radiation condition at infinity.

The problem is solved in the wavenumber domain by the means of a Fourier series decomposition along the circumference of the shell, allowing to express the pressures as a function of the cylindrical harmonics

$$p(r,\theta) = \sum_{n=-\infty}^{\infty} \tilde{p}_n(r) \mathrm{e}^{\mathrm{j}n\theta} \tag{27}$$

The Helmholtz equation can be solved in the wavenumber domain using a linear combination of Bessel functions. As such, the pressure inside the coating, $\tilde{p}^1$, and outside the coating, $\tilde{p}^\infty$, accounting for the previously stated conditions, can be expressed as[35]

$$\tilde{p}^1(r,n) = A_1 \frac{H_n(k_{pr}r)}{H_n(k_{pr}R)} + B_1 J_n(k_{pr}r) H_n(k_{pr}R_1) \quad \text{if} \quad r \leqslant R_1 \tag{28a}$$

$$\tilde{p}^\infty(r,n) = A_\infty \frac{H_n(k_{fr}r)}{H_n(k_{fr}R_1)} + \mathrm{j}^n J_n(k_{fr}r) \quad \text{if} \quad r \geqslant R_1 \tag{28b}$$

where A_n and B_n are the unknowns, J_n and H_n are the Bessel function of the first kind and the Hankel function of the second kind, respectively, R is the radius of the shell, R_1 the exterior radius of the coating, and $k_{ir} = k_i \cos(\theta^i)$ (with k_i the acoustic wavenumber in the domain i). The unknowns can be obtained by considering first the Neumann condition at the shell surface, the continuity of pressures and velocities at the interface between the fluid and the coating, and then solving the subsequent system of equations

$$\begin{bmatrix} -1 & \frac{H_n(k_{pr}R_1)}{H_n(k_{pr}R)} & J_n(k_{pr}R_1)H_n(k_{pr}R_1) \\ -\frac{k_{fr}r}{\rho_f}\frac{H_n'(k_{fr}R_1)}{H_n(k_{fr}R_1)} & \frac{k_{pr}}{\rho_p}\frac{H_n'(k_{pr}R_1)}{H_n(k_{pr}R)} & \frac{k_{pr}}{\rho_p}J_n'(k_{pr}R_1)H_n(k_{pr}R_1) \\ 0 & k_{pr}\frac{H_n'(k_{pr}R)}{H_n(k_{pr}R)} & k_{pr}J_n'(k_{pr}R)H_n(k_{pr}R_1) \end{bmatrix} \begin{bmatrix} A_\infty \\ A_1 \\ B_1 \end{bmatrix} = \begin{bmatrix} \mathrm{j}^n J_n(k_{fr}r) \\ \frac{k_{fr}r}{\rho_f}\mathrm{j}^n J_n'(k_{fr}r) \\ 0 \end{bmatrix} \tag{29}$$

The blocked pressure at the surface of the shell can then be expressed as

$$\tilde{p}_{bloq}(r=R,n) = A_1 + B_1 J_n(k_{pr}R)H_n(k_{pr}R_1) \tag{30}$$

As stated previously, the next step is then to use the expression of Eq. 30 as an excitation term of the cylindrical shell. To do so, the behavior of the shell will be described using the Flügge equations[31,36]

$$\tilde{\mathcal{L}}(n)\begin{bmatrix} \tilde{U}(n) \\ \tilde{V}(n) \\ \tilde{W}(n) \end{bmatrix} = \gamma \begin{bmatrix} 0 \\ 0 \\ \tilde{p}_{bloq}(r=R,n) \end{bmatrix} \tag{31}$$

where $\mathcal{L}$ is the Flügge operator, $\gamma = -\frac{(1-\nu_s^2)R^2}{E_s h_s}$ and U, V and W are the axial, tangential and radial displacements, respectively. The resolution of this system of equations allows expressing the radial displacement as

$$\tilde{W}(n) = -\frac{\gamma\tilde{p}_{bloq}(r=R,n)\left(\tilde{Z}_{UU}(n)\tilde{Z}_{VV}(n) - \tilde{Z}_{UV}^2(n)\right)}{\tilde{\Delta}(n)} \tag{32}$$

with $\tilde{Z}_{ij}$ being the coefficients of the Flügge operator, and $\tilde{\Delta}$ is the determinant of the Flügge matrix taking into account the loading of the fluid and of the coating. It can be expressed as

$$\begin{aligned} \tilde{\Delta} =& \tilde{Z}_{UW}(\tilde{Z}_{UV}\tilde{Z}_{VW} - \tilde{Z}_{UW}\tilde{Z}_{VV}) + \tilde{Z}_{VW}(\tilde{Z}_{UW}\tilde{Z}_{UV} - \tilde{Z}_{VW}\tilde{Z}_{UU}) + \\ & (\tilde{Z}_{WW} + \gamma\tilde{Z}_f)(\tilde{Z}_{UU}\tilde{Z}_{VV} - \tilde{Z}_{UV}^2) \end{aligned} \tag{33}$$

where $\tilde{Z}_f$ is the effective spectral impedance of the fluid and coating. This quantity can be obtained similarly as the blocked pressure in the system of Eq. 29, with the following conditions

- homogeneous Helmholtz equation in the exterior fluid domain and in the coating,
- Sommerfeld radiation condition at infinity.
- Euler equation depending on the radial shell velocity at the shell surface,

- continuity of pressures and velocities at the interface between the fluid and the coating.

The system of equations which must be solved now reads

$$\begin{bmatrix} -1 & \frac{H_n(k_{pr}R_1)}{H_n(k_{pr}R)} & J_n(k_{pr}R_1)H_n(k_{pr}R_1) \\ -\frac{k_{fr}r}{\rho_f}\frac{H_n'(k_{fr}R_1)}{H_n(k_{fr}R_1)} & \frac{k_{pr}}{\rho_p}\frac{H_n'(k_{pr}R_1)}{H_n(k_{pr}R)} & \frac{k_{pr}}{\rho_p}J_n'(k_{pr}R_1)H_n(k_{pr}R_1) \\ 0 & k_{pr}\frac{H_n'(k_{pr}R)}{H_n(k_{pr}R)} & k_{pr}J_n'(k_{pr}R)H_n(k_{pr}R_1) \end{bmatrix} \begin{bmatrix} A_\infty \\ A_1 \\ B_1 \end{bmatrix} = \begin{bmatrix} 0 \\ 0 \\ \rho_p\omega^2 \end{bmatrix} \tag{34}$$

and the fluid and coating loading impedance is obtained

$$\tilde{Z}_f = A_1 + B_1 J_n(k_{pr}R)H_n(k_{pr}R_1) \tag{35}$$

Finally, the shell's radial displacement can be used to obtain the displacement of the external part of the coating, and, subsequently, the pressure reradiated by the shell (using the Euler equation)

$$\tilde{W}_{coat}(n) = \frac{k_{pr}}{\rho_p\omega^2}\left(A_1\frac{H_n'(k_{pr}R_1)}{H_n(k_{pr}R)} + B_1 J_n'(k_{pr}R_1)H_n(k_{pr}R_1)\right)\tilde{W}(n) \tag{36}$$

where A_1 and B_1 are the unknowns obtained when computing the effective fluid and coating impedance in Eq. 34.

In the next sections, the influence of the partial coating will be evaluated via two quantities: the evaluation of the near-field reradiated pressure at the ring frequency of the shell, and the target strength of the shell in the entire frequency spectrum. The target strength is defined as the ratio between the far-field scattered pressure brought back to 1 m from the object, and the incident pressure of the acoustic plane wave.

4.2. *Evaluation of the near-field pressure at the ring frequency*

At first, we are interested in the near-field reradiated pressure at the ring frequency. The ring frequency corresponds to the frequency at which the longitudinal wavelength in the shell is equal to the circumference and is defined as

$$f_r = \frac{1}{2\pi R}\sqrt{\frac{E_s}{\rho_s(1-\nu_s^2)}} \tag{37}$$

Around the ring frequency, the radiation efficiency of the cylindrical shell is particularly high, and this frequency also exhibits a change in behavior of the shell. Indeed, above the ring frequency, it is generally admitted that the cylindrical shell behaves like a plate,[37] in the sense that the flexural motions are mainly decoupled from the longitudinal and shear

motions. It will then be interesting to study the behavior of the partially coated shell at this particular frequency. For the case of interest, the ring frequency yields $f_r = 958$ Hz.

The cartography of the near-field reradiated pressure will be presented for two loading cases, as illustrated in Figure 5. The first one corresponds to an acoustic plane wave having a normal incidence on the missing coating patch ($\theta_i = \frac{\pi}{8}$), while the second one will be directed towards the positive x-axis ($\theta_i = \pi$). For each loading case, a comparison is made between the uncoated shell, the fully coated shell, and the partially coated shell. And for the latter, the results of the coupled CTF-rCTF approach are compared to a reference FEM calculation which has been conducted using COMSOL Multiphysics®. For the FEM calculation, it must be mentioned that the elastic radiated pressure cannot be obtained directly. To obtain this quantity from a FEM calculation, it is necessary to go back to the definition of the radiated pressure given in Eq. 26. As such, the reradiated pressure can be infered by subtracting the blocked pressure from the total pressure. Following this definition, two FEM calculations must be performed: a full calculation accounting for the elastic motion of the shell, and a blocked pressure calculation where the shell is not modelled, in order to be considered as rigid.

The first loading case, corresponding to an incident acoustic plane wave impacting the shell at the location of the missing coating material, is shown in Figure 6. The direction of the incident plane wave is specified in Figure 6a. The first observation that can be made regarding Figures 6a (uncoated shell) and 6b (fully coated shell) is that the anechoic coating has a beneficial impact as the values of the reradiated pressure are globally much lower when the coating is applied on the shell. Then, regarding Figures 6c (FEM reference calculation) and 6d (CTF-rCTF calculation) which show the pressure field for the partially coated shell, we can see that there is a very good agreement between the two calculations, which validates the formulation proposed in Section 2. The different patterns of maxima and minima of pressure are correctly localized, and the amplitudes are well correlated. It can also be said that the absence of coating on the impact area of the plane wave increases the reradiated pressure, especially at the vicinity of the shell, as it could have been expected. Finally, it is important to stress that the symmetry of the system with respect to the angle of incidence of the plane wave has been well complied with.

Concerning the second loading case, corresponding to an acoustic plane wave arriving towards the positive x-axis, the reradiated pressure is shown in Figure 7 for the four configurations. It can be observed that the fully coated shell and the partially coated shell exhibit a very similar behavior. This shows that the partial coating has a very low influence on the behavior of the shell when the missing coating material is located in the shadow area of the shell. This figure also highlights that the CTF-rCTF and FEM calculations exhibit almost the same results, as it was observed in Figure 6 for the previous loading case. This is associated to the previous observation concerning the low impact of the partial coating for this configuration, hence limiting the influence of the sensitivity of the rCTF method.

To conclude on this part, the results presented in this paragraph show that the partial coating can have an impact on the reradiated pressure, compared to the fully coated shell. But this change in behavior is restricted to the case where the incident plane wave impinges

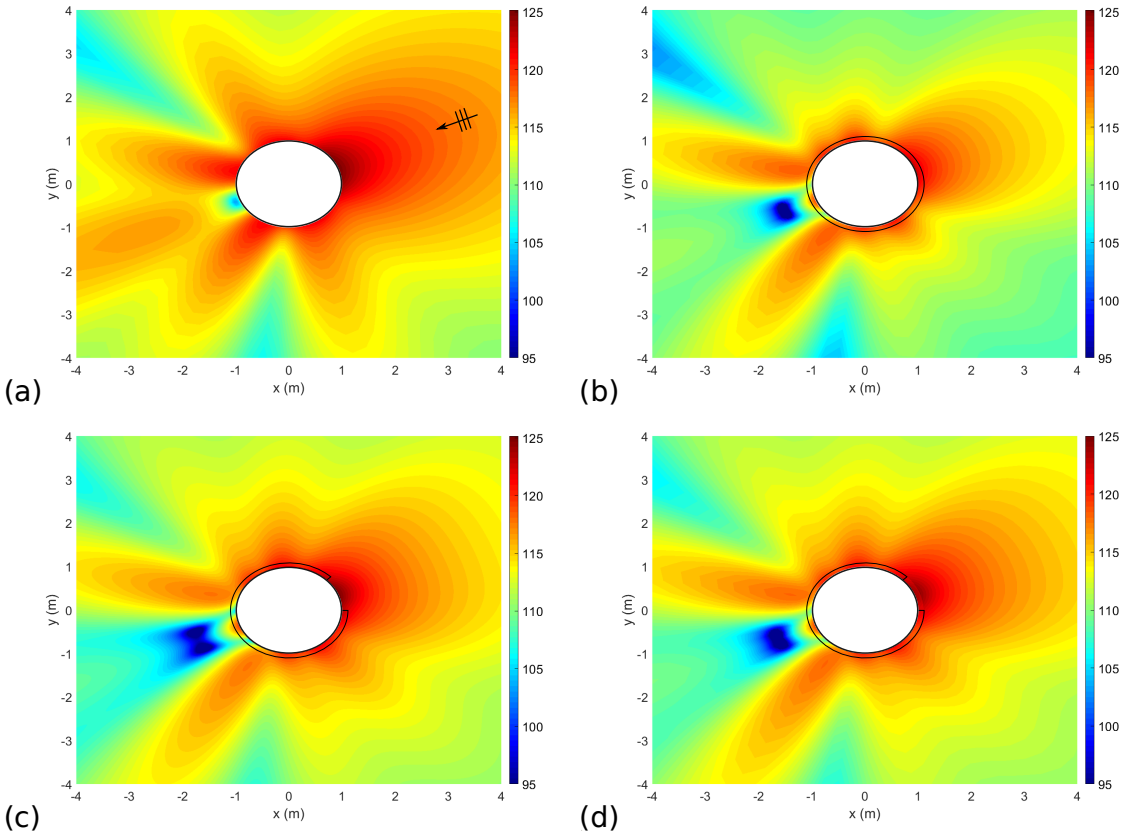

Figure 6. Reradiated pressure (in dB ref. 1e-6 Pa) for $\theta_i = \frac{\pi}{8}$. (a) Uncoated shell. (b) Fully coated shell. (c) Partially coated shell - reference calculation. (d) Partially coated shell - CTF-rCTF calculation.

directly the shell around the uncoated area. When the plane wave is incident on a coated part of the shell, the impact of the partial coating on the reradiated pressure is very limited.

4.3. *Impact of the partial coating on the target strength of the shell*

We are now interested into evaluating the elastic component of the target strength of the shell, and the impact of the partial coating on this quantity, for the two lading configurations. As stated earlier, the target strength is defined as the ratio between the far-field scattered pressure brought back to 1 m from the object, and the incident pressure of the acoustic plane wave. It can be evaluated at the same angle as the incident angle of the plane wave (monostatic target strength) or at a different angle (bistatic target strength). In this study, we are only interested in the monostatic target strength for the two loading cases.

The elastic component of the target strength corresponds to the evaluation of the target strength when only the reradiated pressure p_{rad} is accounted for. In practice, it can be obtained for a 2-D case by using the asymptotic expression of the Hankel function for large

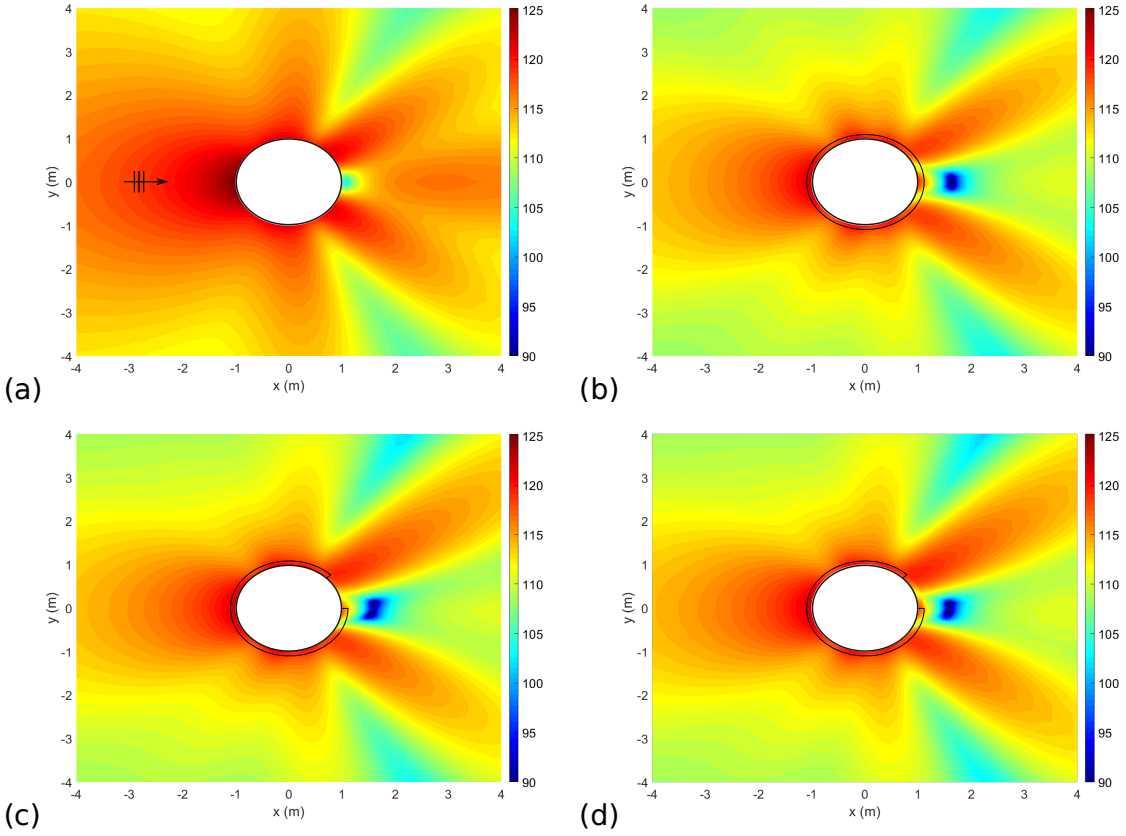

Figure 7. Reradiated pressure (in dB ref. 1e-6 Pa) for $\theta_i = \pi$. (a) Uncoated shell. (b) Fully coated shell. (c) Partially coated shell - reference calculation. (d) Partially coated shell - CTF-rCTF calculation.

arguments. This allows predicting the far-field reradiated pressure from the radial spectral displacement of the shell for uncoated shells, or of the radial spectral displacement of the external boundary of the coating for coated shells. Its expression for a coated shell yields

$$p_{rad}^{far}(r,\theta) = \frac{\rho_f \omega^2}{k_0}\sqrt{\frac{2}{\pi r k_0}}\sum_{n=-\infty}^{n=+\infty}\frac{\tilde{W}_{coat}(n)}{H_n^{(2)'}(R_1 k_0)}\mathrm{e}^{-\mathrm{j}rk_0+\mathrm{j}\frac{(n+1)\pi}{2}+\mathrm{j}n\theta}, \quad r \gg \frac{2\pi}{k_0} \tag{38}$$

where $\tilde{W}_n^{coat}$ is the spectral radial displacement of the external boundary of the coating obtained in Eq. 36, and $H_n^{(2)'}$ is the derivative of the Hankel function of the second kind and of order n. It must be noted that Eq. 38 exhibits an infinite sum. In practice, this sum is truncated to a maximal circumferential order, and the choice of this value is explained in details in.[22]

For the partially coated shell, however, we have seen in Section 2 that the final quantity that is obtained using the CTF-rCTF method is the radiated pressure, and there is no

information concerning the radial displacement of the shell or of the coating. Hence, the far-field pressure will be evaluated in the same way as the near-field pressure, using Eq. 12. To obtain the reradiated far-field pressure, the process is the same as for the FEM calculation. Two calculations are performed to obtain the total pressure and the blocked pressure, and the reradiated pressure is obtained by subtracting the latter from the former. When the far-field reradiated pressure has been computed for all of the coating configurations, the monostatic target strength can be obtained from the following expression

$$TS_{mono}(\theta) = 10\log\left(\frac{\left(\sqrt{r}p_{rad}^{far}(r,\theta)\right)^2}{p_0^2}\right) \tag{39}$$

with p_0 being the amplitude of the incident plane wave.

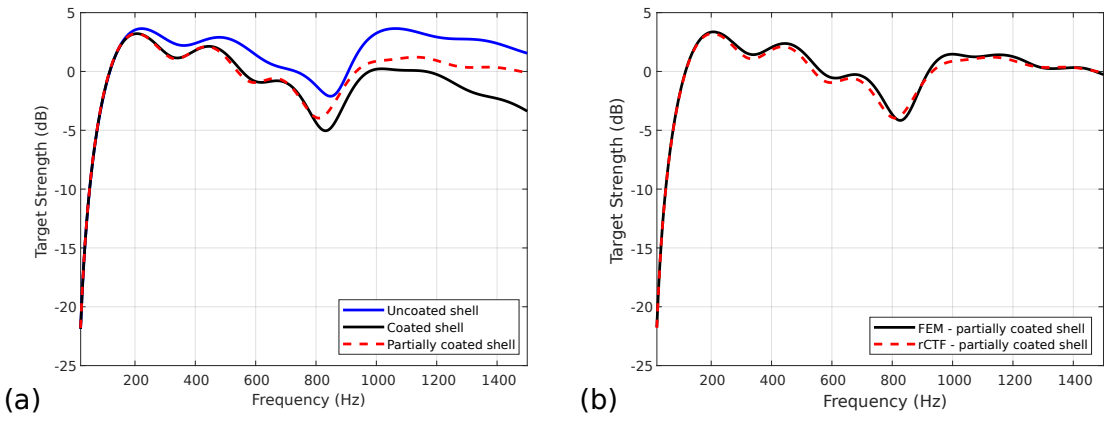

Figure 8. Monostatic target strength when the plane wave is incident on the uncoated part of the shell ($\theta_i = \pi/8$). (a) Comparison between the coating situations. (b) Comparison between the rCTF and FEM calculations.

The monostatic target strength for the three different coating situations (uncoated, fully coated and partially coated) is shown in Figure 8a, for the first loading case (i.e. the acoustic plane wave impinges the missing coating area of the shell). We can observe that the target strength of the uncoated shell is higher than for the fully and partially coated shells, which shows that the anechoic coating also proves its interest when it comes to limiting the scattering in the far-field. It is also interesting to notice that there is not much difference between the fully coated and the partially coated shell up to 800 Hz. Then the target strength tends to be slightly higher for the partially coated shell up to 1200 Hz, and the gap increases for frequencies above 1200 Hz. To analyze this result, one could look for a relation between the size of the opening and the acoustic wavelength in the coating. Indeed, we could assume that, if the acoustic wavelength is greater than the opening, then

the plane wave will be attenuated by the coating nevertheless. With the opening spreading from 0 to $\pi/4$, its length is then $\pi/4$ m (as the shell's radius is 1 m). From this value, we can define a limit frequency f_l above which the acoustic wavelength in the coating will be smaller than the opening. In this case, we obtain f_l=1070 Hz. This is hence consistent with the hypothesis stating that the partial coating will mainly have an impact at frequencies where the acoustic wavelength in the coating is smaller than the opening. Besides, it can be observed in Figure 8b that there is an excellent agreement between the rCTF and the FEM calculations, which is consistant with the previous observations made in Section 4.2 and validates the coupled CTF-rCTF approach.

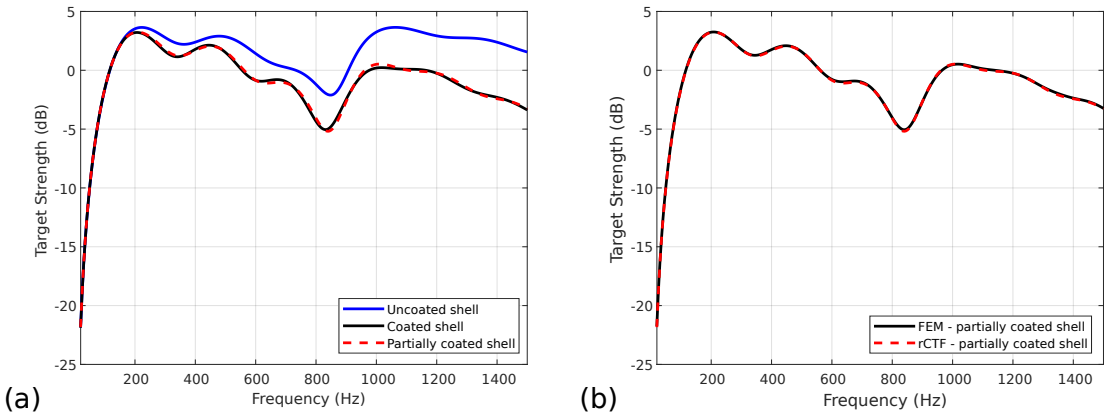

Figure 9. Monostatic target strength when the plane wave is incident on the coated part of the shell ($\theta_i = \pi$). (a) Comparison between the coating situations. (b) Comparison between the rCTF and FEM calculations.

Concerning the second loading case, the comparison between the different coating situations is shown in Figure 9a. The results displayed in this figure are very consistent with the analysis made from Figure 7, which state that the absence of coating on a given part of the shell does not have a significant impact on the scattering of the shell when this specific part is not impinged by the plane wave. Hence, as the behavior of the fully coated and partially coated shells are similar for this loading case, the CTF-rCTF exhibits no calculation error compared to the FEM calculation. The conclusions drawn in this study will have to be investigated in more details in further studies, and particularly for 3D stiffened cylindrical shells for which very specific scattering phenomena can be observed.

5. Conclusion

In this paper, the scattering problem of an acoustic plane wave by a partially coated cylindrical shell has been addressed using the CTF and rCTF methods. The theoretical fundamentals of the method which were previously developed for studying radiation problems have been extended in the present paper to the case of scattering problems. A theoretical

framework for the calculation of elastic radiated pressure and elastic target strength has been proposed for the cases of fully coated and partially coated cylindrical shells.

A comparison with FEM simulations on a 2D model validates the proposed coupled CTF-rCTF approach, while it is expected that the latter will require much less computing time to deal with 3D models than with a FEM simulation. The comparison with the FEM calculation exhibits accurate results for both the near-field pressure and the far-field pressure (represented by the elastic target strength). These first results show that the influence of the partial coating is particularly highlighted when the incident acoustic plane wave is heading towards the area where the coating material is missing, and for frequencies where the acoustic wavelength in the coating is smaller than the opening.

It is important to mention that these results, although giving a first insight into the possibilities brought by the rCTF method, are not completely of interest for naval applications, as the calculations were performed on a 2D model of an unstiffened shell. However, this study must be seen as a first step towards the possibility of studying the scattering from a 3D partially coated, stiffened cylindrical shell.

Acknowledgements

This work was funded by the French National Research Agency (ANR) within the plan "France Relance", and was performed within the framework of the LabEx CeLyA (ANR-10-LABX-0060) of Université de Lyon, in collaboration with Naval Group Research.

Bibliography

1. E. A. Skelton and J. H. James, *Theoretical acoustics of underwater structures* (Imperial College Press, London : River Edge, NJ, 1997).
2. B. Laulagnet and J. L. Guyader, Sound radiation from a finite cylindrical shell covered with a compliant layer, *J. Vib. Acoust.* **113** (1991) 267–272.
3. J. M. Cuschieri and D. Feit, Influence of circumferential partial coating on the acoustic radiation from a fluid-loaded shell, *J. Acoust. Soc. Am.* **107** (2000) 3196–3207.
4. B. Laulagnet and J. L. Guyader, Sound radiation from finite cylindrical coated shells, by means of asymptotic expansion of three-dimensional equations for coating, *J. Acoust. Soc. Am.* **96** (1994) 277–286.
5. J. M. Cuschieri, The modeling of the radiation and response Green's function of a fluid-loaded cylindrical shell with an external compliant layer, *J. Acoust. Soc. Am.* **119** (2006) 2150–2169.
6. G. S. Sharma, A. Skvortsov, I. MacGillivray and N. J. Kessissoglou, Acoustic performance of gratings of cylindrical voids in a soft elastic medium with a steel backing, *J. Acoust. Soc. Am.* **141** (2017) 4694–4704.
7. M. Dana, J. Bernard and L. Maxit, A spectral global matrix method for modelling the response of a fluid-loaded multilayered cylindrical shell excited by an acoustic plane wave, *J. Acoust. Soc. Am.* **148** (2020) 2997–3013.
8. G. S. Sharma, A. Skvortsov, I. MacGillivray and N. J. Kessissoglou, Acoustic performance of periodic steel cylinders embedded in a viscoelastic medium, *J. Sound Vib.* **443** (2019) 652–665.
9. G. S. Sharma, A. Skvortsov, I. MacGillivray and N. J. Kessissoglou, Sound absorption by rubber coatings with periodic voids and hard inclusions, *Appl. Acoust.* **143** (2019) 200–210.

10. G. S. Sharma, A. Marsick, L. Maxit, A. Skvortsov, I. MacGillivray and N. J. Kessissoglou, Acoustic radiation from a cylindrical shell with a voided soft elastic coating, *J. Acoust. Soc. Am.* **150** (2021) 4308–4314.
11. S. M. Ivansson, Sound absorption by viscoelastic coatings with periodically distributed cavities, *J. Acoust. Soc. Am.* **119** (2006) 3558–3567.
12. S. M. Ivansson, Numerical design of Alberich anechoic coatings with superellipsoidal cavities of mixed sizes, *J. Acoust. Soc. Am.* **124** (2008) 12.
13. S. M. Ivansson, Anechoic coatings obtained from two- and three-dimensional monopole resonance diffraction gratings, *J. Acoust. Soc. Am.* **131** (2012) 2622–2637.
14. B. Laulagnet and J. Guyader, Sound radiation from finite cylindrical shells, partially covered with longitudinal strips of compliant layer, *J. Sound Vib.* **186** (1995) 723–742.
15. S.-X. Liu, M.-S. Zou, L.-W. Jiang and X.-Y. Zhao, Vibratory response and acoustic radiation of a finite cylindrical shell partially covered with circumferential compliant layers, *Appl. Acoust.* **141** (2018) 188–197.
16. M. Ouisse, L. Maxit, C. Cacciolati and J.-L. Guyader, Patch transfer function as a tool to couple linear acoustic problems, *J. Vib. Acoust.* **127** (2005) pp. 458–466.
17. G. Veronesi, C. Albert, E. Nijman, J. Rejlek and A. Bocquillet, Patch transfer function approach for analysis of coupled vibro-acoustic problems involving porous materials, in *SAE Technical Paper* (2014), pp. 2014–01–2092.
18. J. Rejlek, G. Veronesi, C. Albert, E. Nijman and A. Bocquillet, A combined computational-experimental approach for modelling of coupled vibro-acoustic problems, in *SAE 2013 Noise and Vibration Conference and Exhibition* (2013), pp. 2013–01–1997.
19. M. Aucejo, L. Maxit, N. Totaro and J.-L. Guyader, Convergence acceleration using the residual shape technique when solving structure–acoustic coupling with the Patch Transfer Functions method, *Comput. Struct.* **88** (2010) 728–736.
20. L. Maxit, M. Aucejo and J.-L. Guyader, Improving the Patch Transfer Function approach for fluid-structure modelling in heavy fluid, *J. Vib. Acoust.* **134** (2012) 051011.
21. L. Maxit and J.-M. Ginoux, Prediction of the vibro-acoustic behavior of a submerged shell non periodically stiffened by internal frames, *J. Acoust. Soc. Am.* **128** (2010) 137–151.
22. L. Maxit, Scattering model of a cylindrical shell with internal axisymmetric frames by using the Circumferential Admittance Approach, *Appl. Acoust.* **80** (2014) 10–22.
23. V. Meyer, L. Maxit, J.-L. Guyader, T. Leissing and C. Audoly, A condensed transfer function method as a tool for solving vibroacoustic problems, *Proceedings of the Institution of Mechanical Engineers, Part C: Journal of Mechanical Engineering Science* **230** (2016) 928–938.
24. V. Meyer, L. Maxit, J.-L. Guyader and T. Leissing, Prediction of the vibroacoustic behavior of a submerged shell with non-axisymmetric internal substructures by a condensed transfer function method, *J. Sound Vib.* **360** (2016) 260–276.
25. V. Meyer, L. Maxit and C. Audoly, A substructuring approach for modeling the acoustic scattering from stiffened submerged shells coupled to non-axisymmetric internal structures, *J. Acoust. Soc. Am.* **140** (2016) 1609–1617.
26. F. Dumortier, L. Maxit and V. Meyer, Vibroacoustic subtractive modeling using a reverse condensed transfer function approach, *J. Sound Vib.* **499** (2021) 115982.
27. F. Dumortier, L. Maxit and V. Meyer, Subtractive modelling using the reverse condensed transfer function method: influence of the numerical errors, in *Proceedings of InterNoise 2021* (Washington DC, USA, 2021), p. 12.
28. F. Dumortier, V. Meyer and L. Maxit, A global decoupling technique for subtractive modelling on acoustic and vibration problems, *J. Sound Vib.* **569** (2024) 117969.
29. F. J. Fahy, Some applications of the reciprocity principle in experimental vibroacoustics, *Acoust. Phys.* **49** (2003) 217–229.

30. C. Marchetto, L. Maxit, O. Robin and A. Berry, Vibroacoustic response of panels under diffuse acoustic field excitation from sensitivity functions and reciprocity principles, *J. Acoust. Soc. Am.* **141** (2017) 4508–4521.
31. D. G. Karczub, Expressions for direct evaluation of wave number in cylindrical shell vibration studies using the Flügge equations of motion, *J. Acoust. Soc. Am.* **119** (2006) 3553–3557.
32. M. Nijhof, L. Fillinger, L. Gilroy, J. Ehrlich and I. Schäfer, BeTSSi II : Submarine target strength modeling workshop, in *Proceedings of UACE2017* (Skiathos, Greece, 2017).
33. F. Dumortier, Principle of vibroacoustic subtractive modelling and application to the prediction of the acoustic radiation of partially coated submerged cylindrical shells, Ph.D. thesis, INSA de Lyon, 2021.
34. R. Liétard, D. Décultot, G. Maze and M. Tran-Van-Nhieu, Acoustic scattering from a finite cylindrical shell with evenly spaced stiffeners: Experimental investigation, *J. Acoust. Soc. Am.* **118** (2005) 2142–2146.
35. D. C. Ricks and H. Schmidt, A numerically stable global matrix method for cylindrically layered shells excited by ring forces, *J. Acoust. Soc. Am.* **95** (1994) 3339–3349.
36. W. Flügge, *Statik und dynamik der schalen* (Springer, 1962).
37. M. Heckl, Vibrations of point-driven cylindrical shells, *J. Acoust. Soc. Am.* **34** (1962) 1553–1557.